Seed Biology

ARTICLE

Open Access

https://doi.org/10.48130/seedbio-0024-0014

Seed Biology **2024**, 3: e015

Arabidopsis actin-depolymerizing factor10 depolymerizes apical actin filaments to facilitate pollen tube turning in response to female attractant

Yanan Xu, Jiahao Jiang and Shanjin Huang*

Center for Plant Biology, School of Life Sciences, Tsinghua University, Beijing 100084, China

* Corresponding author, E-mail: sjhuang@mail.tsinghua.edu.cn

Abstract

Peptide/receptor-like kinase-mediated signaling plays a pivotal role in male-female interactions, particularly in guiding the growth of pollen tubes, which is essential for fertilization in flowering plants. However, the downstream cellular events within the pollen tube guidance signaling network remain largely unexplored. In this study, actin dynamics in pollen tubes growing semi-*in vitro* were directly visualized, and it was discovered that AtLURE1s-induced pollen tube growth guidance is intricately regulated by actin assembly and disassembly. The observations revealed that apical actin filaments undergo a process of rapid depolymerization and repolymerization at the leading side, which in turn facilitates the reconstruction of the apical actin structure, enabling the pollen tube to grow in a new direction. Notably, it was observed that actin depolymerization and subsequent repolymerization occur on the leading side before any morphological changes in the pollen tube. Furthermore, it was found that the loss of function of ADF10 results in the accumulation of apical actin filaments, altering the turning behavior of the pollen tube. These findings suggest that rapid actin depolymerization at the leading side and the subsequent reconstruction of the apical structure occur early and are crucial for successful pollen tube turning.

Citation: Xu Y, Jiang J, Huang S. 2024. *Arabidopsis* actin-depolymerizing factor10 depolymerizes apical actin filaments to facilitate pollen tube turning in response to female attractant. *Seed Biology* 3: e015 https://doi.org/10.48130/seedbio-0024-0014

Introduction

Pollen tube growth serves as a conduit for two immotile sperm cells, enabling double fertilization in flowering plants. Throughout their lengthy journey to the ovules, pollen tubes continuously alter their growth direction in response to signals emanating from the female tissues[1]. To successfully navigate to their destination, pollen tubes have evolved intricate systems known as pollen tube guidance mechanisms, which regulate the directionality of tip growth. This guidance is categorized into preovular and ovular guidance[2,3]. Within this framework of male-female interaction, it is widely recognized that female tissues secrete pollen tube attractant peptides. These attractant peptides are perceived by membrane-anchored receptor-like kinases in pollen tubes, triggering downstream cellular events that steer the pollen tubes' direction[4,5]. Among them, defensin-like CRPs, such as LUREs, are well-characterized. LUREs were originally discovered in *Torenia fournieri*[6], and then in *Arabidopsis* and its relatives[7–9]. To date, however, the downstream cellular events triggered by LURE signaling during pollen tube guidance remains largely unexplored.

The successful redirection of pollen tubes relies on the efficient transportation of materials essential for cell wall synthesis and membrane expansion to the newly expanding regions of the pollen tubes[10–12]. Therefore, pollen tube growth guidance is intimately linked to the rapid tip growth of the pollen tubes. In this context, an exocytosis-centered mechanism has been proposed to bridge the gap between pollen tip growth and guided pollen tube growth[13]. Actin dynamics play a pivotal role in polarized pollen tube growth by orchestrating the trafficking of exo- and endocytotic vesicles[14–21]. For instance, perturbation in actin dynamics resulting from the alteration in the function of pollen-expressed actin and its binding proteins influences the growth and morphogenesis of pollen tubes[22–38]. It is evident that actin dynamics are crucial in connecting pollen tube tip growth with guided pollen tube growth. Indeed, previous visualization studies of the actin cytoskeleton in pollen tubes growing *in vitro* have revealed a process of depolymerization and repolymerization at the apical region, which facilitates the reconstruction of the apical structure to support growth in a new direction[39]. However, considering that *in vitro*-grown pollen tubes exhibit random turning, it remains uncertain whether these turning events share similar underlying cellular mechanisms with those observed in pollen tubes guided by external cues.

To address this question, a semi-*in vitro* pollen tube growth system was employed combined with advanced live cell imaging techniques to monitor actin filament dynamics during the turning of pollen tubes. The present findings demonstrate that actin filaments undergo rapid depolymerization at the leading side of the pollen tube tip, followed by repolymerization from the plasma membrane, enabling the reconstruction of the apical actin structure and guiding pollen tube growth towards a new direction. Notably, it was observed that the reconstruction of the apical actin structure precedes morphological changes in the pollen tubes, suggesting that it is an early cellular event

during guided pollen tube growth. Furthermore, by analyzing the effect of loss of function of *Arabidopsis* actin-depolymerizing factor 10 (ADF10)[40], the present study specifically reveals that actin depolymerization at the leading side of the turning pollen tube is crucial for successful turning. This process appears to be essential for the pollen tube to respond to external cues, such as female-derived peptides. By elucidating these cellular mechanisms, we gain insights into how pollen tubes can navigate and grow towards their target, providing valuable insights into the intricate link between pollen tube tip growth and guidance.

Materials and methods

Plant materials and growth conditions

The information for the *Arabidopsis ADF10* TALEN line has been described previously[40]. The *Arabidopsis ADF10* CRISPR line was generated according to the method described below. The information of *FIM5pro:FIM5-EGFP;fim5* plants and *FH5pro:FH5-EGFP;fh5* plants can be found in previously published papers[26,29]. The *Arabidopsis thaliana* Columbia ecotype (Col-0) was used as a wild type. The *Arabidopsis thaliana* plants were grown at 22 °C under a photoperiod of 16-h-light/8-h-dark in soil within a growth room.

Generation of *ADF10* loss-of-function CRISPR lines

Two guide RNAs specific to *ADF10* were ligated into the vector PHEE401 according to the method described previously[41]. The constructed ADF10 CRISPR vector was transformed into *Agrobacterium* strain GV3101, which was subsequently used to transform wild-type plants *via* the floral dip method[42]. Genomic DNA was extracted from the T1-transgenic plants, and fragments surrounding the ADF10 target sites were amplified using the primers ADF10-CRISPR-F (5'-CGACGTATC AGTGTTGTGAC-3') and ADF10-CRISPR-R (5'-CGAAAGTGAGCTA TTACACG-3'). These PCR products were then sequenced to identify mutations in the *ADF10* gene. From the sequenced plants, homozygous *ADF10* knockout lines were selected. These lines were propagated to obtain T2 seeds. Genomic DNA from T2 plants was extracted, and primers Zcas9-IDF32 (5'-CTGTTCGTCGAGCAGCACAAGCATT-3') and tE9-IDR (5'-CATT AGAGGCCACGATTTGACACAT-3') were used to identify non-transgenic plants (those without the CRISPR construct). Finally, the non-transgenic *ADF10* knockout mutants from the T2 generation were propagated to obtain T3 seeds. These T3 non-transgenic *ADF10* knockout mutants were then used for further experiments.

Protein purification

To generate AtLURE1.2 peptides, the coding sequences of AtLURE1.2 were fused with a His-tag at the C-terminal using the pET28a vector. This construct was then transformed into *E. coli* BL21 (DE3) cells. Once the optical density (OD) at 600 nm reached 0.6, the cells were induced to express the protein by adding 0.5 mM isopropyl-β-d-thiogalactopyranoside (IPTG). This induction was maintained for 4 h at 37 °C and the bacterial cells were subsequently harvested by centrifugation and resuspended in a buffer containing 5 mM imidazole (pH 7.0). This suspension was then lysed using sonication to release the intracellular proteins. After centrifugation at 1,935 *g* for 15 min, the pellets containing insoluble protein fractions were collected. This centrifugation and pellet collection step was repeated three times. The insoluble AtLURE1.2-His peptides, trapped within the inclusion bodies, were solubilized overnight at 4 °C in a buffer containing 50 mM tris, 50 mM glycine, 8 M urea, and 1 mM β-mercaptoethanol (pH 8.0). Following solubilization, the mixture was centrifuged at 1,935 *g* for 15 min to remove any remaining insoluble debris. The supernatants containing the solubilized peptides were then refolded over 5 d at 4 °C using a buffer system containing tris, L-Arginine, PMSF, and urea. After refolding, the peptides were dialyzed against 10 mM Tris-HCl (pH 8.0), and the dialyzed peptides were purified using Ni-NTA affinity chromatography, following the manufacturer's instructions. Finally, the purified protein was dialyzed against 5 mM Tris-HCl (pH 8.0).

Semi-*in vitro* AtLURE1.2-responsive assay

Three previously used pollen germination mediums (PGMs) were employed to investigate the growth of semi-*in vitro* pollen tubes, designated as 1#PGM, 2#PGM, and 3#PGM. Each medium was specifically designed to provide different nutritional and ionic conditions for pollen germination and tube growth. For instance, 1#PGM contains 1 mM $Ca(NO_3)_2$, 1 mM $CaCl_2$, 1 mM $MgSO_4$, 0.01% (w/v) H_3BO_3, 18% (w/v) sucrose, and 1.5% (w/v) low-melting agarose, pH 6.9–7.0[26]. 2#PGM, on the other hand, contains 1.27 mM $Ca(NO_3)_2$, 0.4 mM $MgSO_4$, 0.001% (w/v) H_3BO_3, 14% (w/v) sucrose, and 1.5% (w/v) low-melting agarose, pH 7.0[43]. Lastly, 3#PGM comprises 5 mM $CaCl_2$, 5 mM KCl, 1 mM $MgSO_4$, 0.01% (w/v) H_3BO_3, 10% (w/v) sucrose, and 1.5% (w/v) low-melting agarose, pH 7.5[44]. The semi-*in vitro* AtLURE1.2-responsive assay was then conducted to visualize the wavy tip growth of pollen tubes attracted by AtLURE1.2, following the previously described protocol[4]. This assay involved adding purified AtLURE1.2 peptides to the melted PGM, whether it be 1#PGM, 2#PGM, or 3#PGM. Once the PGM solidified, it was cut into small squares and placed on a glass slide. The wild-type pistils were emasculated the night before, and pollen derived from either wild-type or *adf10* mutant plants was pollinated onto these pistils. Approximately one hour after hand-pollination, the styles were excised using a needle and placed on the solid PGM containing AtLURE1.2 peptides. The excised styles were then incubated at 22 °C for 4–6 h before observation under an Olympus BX53 microscope equipped with a 20× objective lens and a CCD camera. Quantification of pollen tube morphology was performed using ImageJ software, allowing for quantitative analysis of the effects of AtLURE1.2 on pollen tube growth in the different PGMs.

LURE beads guidance assay

Semi-*in vitro* pollen tubes grow on the PGM in the absence of AtLURE1.2 peptides, as described previously[4]. To investigate the pollen tube's directed attraction towards AtLURE1.2, the LURE1 beads guidance assay was performed according to the method described previously[5]. An equal volume of purified AtLURE1.2 peptides were mixed with 12% (w/v) gelatin and subsequently added into 150 μL silicone oil (viscosity 100cSt; SIGMA-ALDRICH). This mixture was then vortexed to divide it into small beads. The beads were placed obliquely in front of the pollen tube tip using an Olympus CKX53 micro-manipulator mounted on an inverted microscope. The growing process of pollen tubes toward the beads was observed under an Olympus CX21 microscope equipped with a 10× objective lens and was captured by a CCD camera.

Pharmacological treatments

To investigate the impact of latruculin B (LatB) on pollen germination, various concentrations of LatB were first mixed

into molten solid PGM1# maintained at 40 °C. Then, pollen grains harvested from WT, the *ADF10* loss-of-function CRISPR line 95#-14, and the TALEN line #10 were deposited onto the PGM surface containing these different concentrations of LatB. After deposition, the samples were incubated at 28 °C for 3 h to allow germination to occur. The germination process was closely monitored using an Olympus CX21 microscope with a 10× objective lens, and the images were captured using a CCD camera. Following the incubation period, a quantitative analysis of pollen germination rates was conducted using ImageJ software, taking into account the various LatB concentrations.

Visualization of actin filaments, FIM5, and ADF10 subcellular localization in living pollen tubes

To visualize the dynamics of apical actin filaments, pollen tubes expressing Lifeact-EGFP were utilized, as described by Qu et al.[45]. Similarly, for the observation of the spatiotemporal subcellular distribution of FIM5 and ADF10, pollen tubes derived from *FIM5pro:FIM5-EGFP;fim5*[26] and *ADF10pro:ADF10-EGFP;adf10*[40] were employed, respectively. These pollen tubes were grown on solid PGM containing 5 μM AtLURE1.2 peptides and passed through the cut style, as previously described. Once most pollen tubes had grown to a length of 200–300 μm on the PGM, the PGM was inverted and placed in a confocal dish. Subsequently, the time-lapse imaging was performed using a spinning disk confocal microscope equipped with an 100× oil objective lens. Z-stack time series images were acquired at 3-s intervals, with the z-steps set at 0.7 μm. The collected images were then analyzed using ImageJ software.

Analysis of the fluorescence intensity of actin filaments and the turning angles of pollen tubes

To quantify the content of actin filaments at the pollen tube tip, ImageJ software was used to measure the fluorescence intensity of Lifeact-EGFP at the apical region 2.5–3.5 μm away from the tip. Specifically, a 1 μm wide straight line was drawn precisely 2.5 μm from the tip. Utilizing the 'Plot Profile' plugin in ImageJ, the gray value of each point along this line was measured and plotted the data as a curve. Similarly, the fluorescence intensity of FIM5-EGFP was analyzed at the regions 3.5–4.5 μm and 2.5–3.5 μm from the tip. To assess the relative abundance of actin filaments on both the leading and rear sides, the pollen tube was divided into two sections along its growth axis and the mean gray value of each section was measured independently using ImageJ. Finally, to determine the turning angle of the pollen tubes, ImageJ was employed to calculate the included angle between the initial and new growth directions. This included angle served as a metric for quantifying the degree of tube turning.

Results

Apical actin filaments undergo rapid depolymerization and repolymerization at the leading side during AtLURE1.2-induced tube turning

A semi-*in vitro* assay was developed that responds to AtLURE1.2, as previously reported by Takeuchi & Higashiyama[4], to visually observe the behavior of the actin cytoskeleton within pollen tubes as they are directed to grow by female-emitted signals. To optimize the growth state of pollen tubes grown outside the cut style, three germination mediums were initially tested: 1#, 2#, and 3#, as reported in the literature. It was discovered that pollen tubes grew with the fastest velocity on the 3#PGM, both in the presence and absence of AtLURE1.2 (Supplemental Fig. S1). Therefore, the 3# medium was selected for subsequent experiments. In contrast to pollen tubes that grew straight in the absence of AtLURE1.2, the presence of various concentrations of AtLURE1.2 induced a wavy growth pattern in pollen tubes (Supplemental Fig. S2a). In support of the notion that this is a specific response to AtLURE1.2, it was observed that *prk6* pollen tubes grew straightly, even in the presence of AtLURE1.2 (Supplemental Fig. S2a[4]). Consistent with this, it was found that pollen tubes grew straight *in vitro* when exposed to AtLURE1.2 (Supplemental Fig. S2b).

Next, pollen tubes expressing *Lat52::Lifeact-EGFP*[45,46] were visualized growing semi-*in vitro*. Initially, it was demonstrated that pollen tubes harboring Lifeact-EGFP exhibited a wavy growth pattern (Fig. 1a), indicating their responsiveness to AtLURE1.2. Utilizing spinning disk confocal microscopy, it was observed the dynamics of actin filaments in pollen tubes as they turned in response to AtLURE1.2. The focus was on monitoring the dynamics of apical actin filaments, which have been shown to undergo rapid changes during re-orientation in pollen tubes growing *in vitro*[39]. It was observed that the actin filaments at the leading side underwent a process of rapid depolymerization followed by gradual repolymerization, allowing for the reestablishment of the apical actin structure (Fig. 1b, c).

To reveal the changes in actin dynamics with higher spatiotemporal resolution during wavy pollen tube growth, we sought to trace the alterations in the actin cytoskeleton within pollen tubes as they turn. Initially, the changes in angles formed between the new growth axis and the original growth axis of pollen tubes (Fig. 1d) were quantified and plotted the fluorescence intensity of actin filaments on both sides of the pollen tubes and the angles during the turning process. The findings indicate that actin filaments undergo depolymerization and repolymerization at the leading side, whereas no significant change in the amount of actin filaments was observed at the rear side of the pollen tubes (Fig. 1e). To eliminate the possibility of artifacts arising from the use of the exogenous Lifeact-EGFP marker, actin filaments were also visualised in pollen tubes derived from *FIM5pro:FIM5-EGFP;fim5* plants[26]. This is because FIM5-EGFP effectively labels actin filaments within the growth domain of pollen tubes[47]. It was initially confirmed that the *FIM5pro:FIM5-EGFP;fim5* pollen tubes respond to AtLURE1.2 (Supplemental Fig. S3a). Subsequently, it was discovered that the FIM5-EGFP-labeled actin filaments undergo a similar process of depolymerization and repolymerization at the leading side in the pollen tube (Supplemental Fig. S3b–e), albeit exhibiting a slightly different overall pattern compared to Lifeact-labeled actin filaments. Notably, it was observed that the depolymerization and repolymerization of actin filaments at the leading side preceded the morphological changes in the pollen tubes (Fig. 1e; Supplemental Fig. S3e). This suggests that the rapid depolymerization and subsequent repolymerization of actin filaments at the leading side, to rebuild the apical actin structure towards the future growth direction is an early event during the turning of pollen tubes.

Loss of function of ADF10 affects AtLURE1.2-induced turning behavior of pollen tubes

To understand the molecular mechanism underlying the changes in actin at the leading side of pollen tubes during their

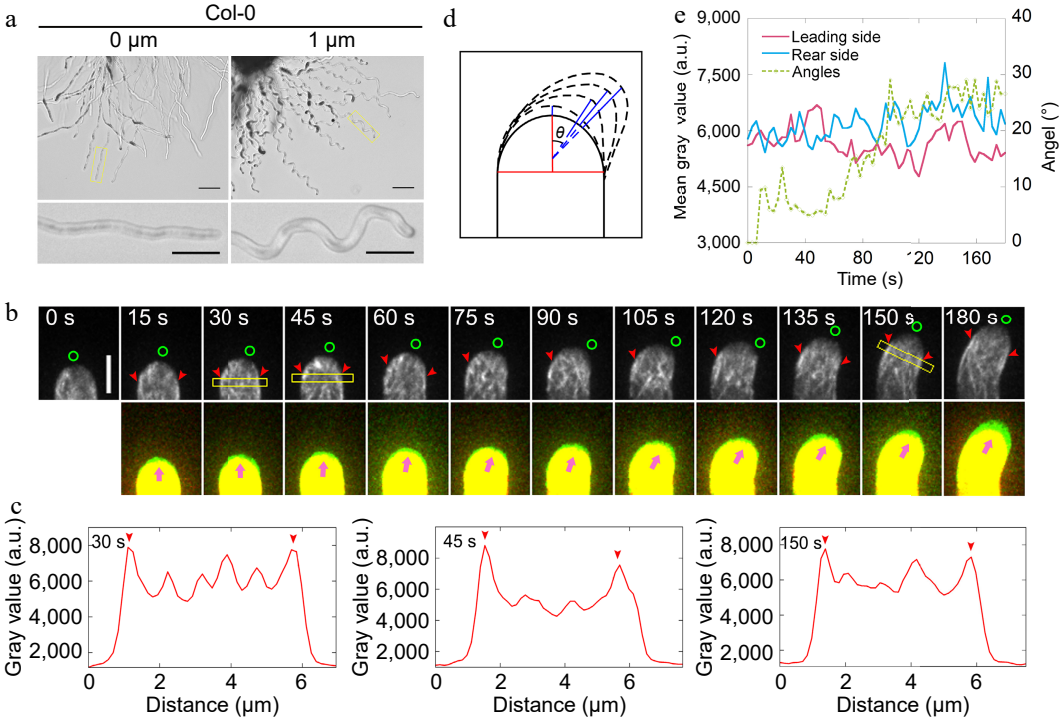

Fig. 1 Actin filaments undergo depolymerization and repolymerization at the leading side of the pollen tube during AtLURE1.2-induced turning. (a) Semi-*in vitro* AtLURE1.2-responsive wavy assay for wild-type (Col-0) 4–6 h after pollination (HAP). The pollen tubes of wild-type show wavy tip growth on the solid PGM containing 1 μM AtLURE1.2 peptides. Scale bars, 50 μm (top) and 20 μm (bottom). The micrographs are representative of three samples. (b) Time-lapse images of actin filaments during AtLURE1.2-induced turning of a semi-*in vitro* growth wild-type pollen tube. The lower panel shows the merged images from two time points, in which the newly grown portion of pollen tubes between two time points was green colored. Green circles in the upper panel and pink arrowheads in the lower panel indicate the pollen tube growth direction, red arrowheads indicate the cortical apical actin filaments. Scale bar, 5 μm. (c) Quantification of the fluorescence intensity of apical actin filaments within yellow boxed square in (b). Red arrowheads indicate the peaks of fluorescence. (d) Schematic describing the quantification of the turning angles. The red vertical line shows the initial tube growth direction and the blue lines show the new growth direction, θ is the included angle of each blue line with the red line, θ change indicates the turning of the pollen tube. (e) Analysis of the fluorescence intensity of the pollen tube in (b) on both sides of the top region 2.5 to 3.5 μm away from the tip and the tube turning over time.

turning, it was examined whether ADF is involved in this process. ADF10 has been identified as crucial for the turnover of subapical actin filaments in pollen tubes, facilitating their depolymerization and severing[40]. Therefore, it was hypothesized that ADF10 might play a role in the turning behavior of pollen tubes. To test this, it was initially investigated whether the loss of function of ADF10 might impact AtLURE1.2-induced pollen tube turning. The growth of *adf10-1* pollen tubes were traced and compared side-by-side with WT pollen tubes. The observations revealed that, although *adf10-1* pollen tubes were able to respond to AtLURE1.2, their morphology differed significantly from that of WT, exhibiting irregular turning patterns (Fig. 2a). Furthermore, another mutant allele of *ADF10*, *adf10-2*, generated using the CRISPR/Cas9 gene editing approach, exhibited similar irregular turning behavior (Supplemental Fig. S4), confirming that this phenotype is indeed a result of the loss of function of *ADF10*. To quantitatively analyze this phenotype, the distance between adjacent peaks and the amplitude of each turn were measured (Fig. 2b top). The analysis revealed that both the distance between adjacent peaks and the amplitude of each turn were reduced in *adf10-1* pollen tubes compared to WT (Fig. 2b bottom; Supplemental Fig. S4e). To gain a deeper understanding of the pollen tube turning behavior, the dynamic turning process was monitored over several consecutive turns and found that the turns in *adf10-1* were smaller compared to WT (Fig. 2c). This could explain why, despite growing slower, *adf10-1* pollen tubes took a shorter time to complete a turn compared to WT (Fig. 2d). Interestingly, it was also observed that *adf10-1* pollen tubes occasionally exhibited non-horizontal turning patterns, resembling spiral growth (Fig. 2c).

To further investigate whether the small and unsmooth wavy tip growth is indeed induced by AtLURE1.2, a LURE1 beads guidance assay was established, as previously reported[5]. The results demonstrated that both *adf10-1* and WT pollen tubes can be attracted by AtLURE1.2 beads. However, there were notable differences in their growth patterns. Specifically, the *adf10-1* tube exhibited a small and unsmooth turning track in comparison to the WT (Fig. 2e, 2f; Supplemental Videos S1–S2). Despite these differences in growth tracks, it was unexpectedly found that *adf10-1* and WT pollen tubes demonstrated similar capabilities in responding to the attraction of AtLURE1.2 beads. This similarity was evident from the data showing that an identical percentage of both *adf10-1* and WT pollen tubes were attracted by AtLURE1.2 beads (Fig. 2e). Collectively, the findings suggest that the loss-of-function of ADF10 alters the AtLURE1.2-induced tube turning behavior, while maintaining a comparable response to the attractant.

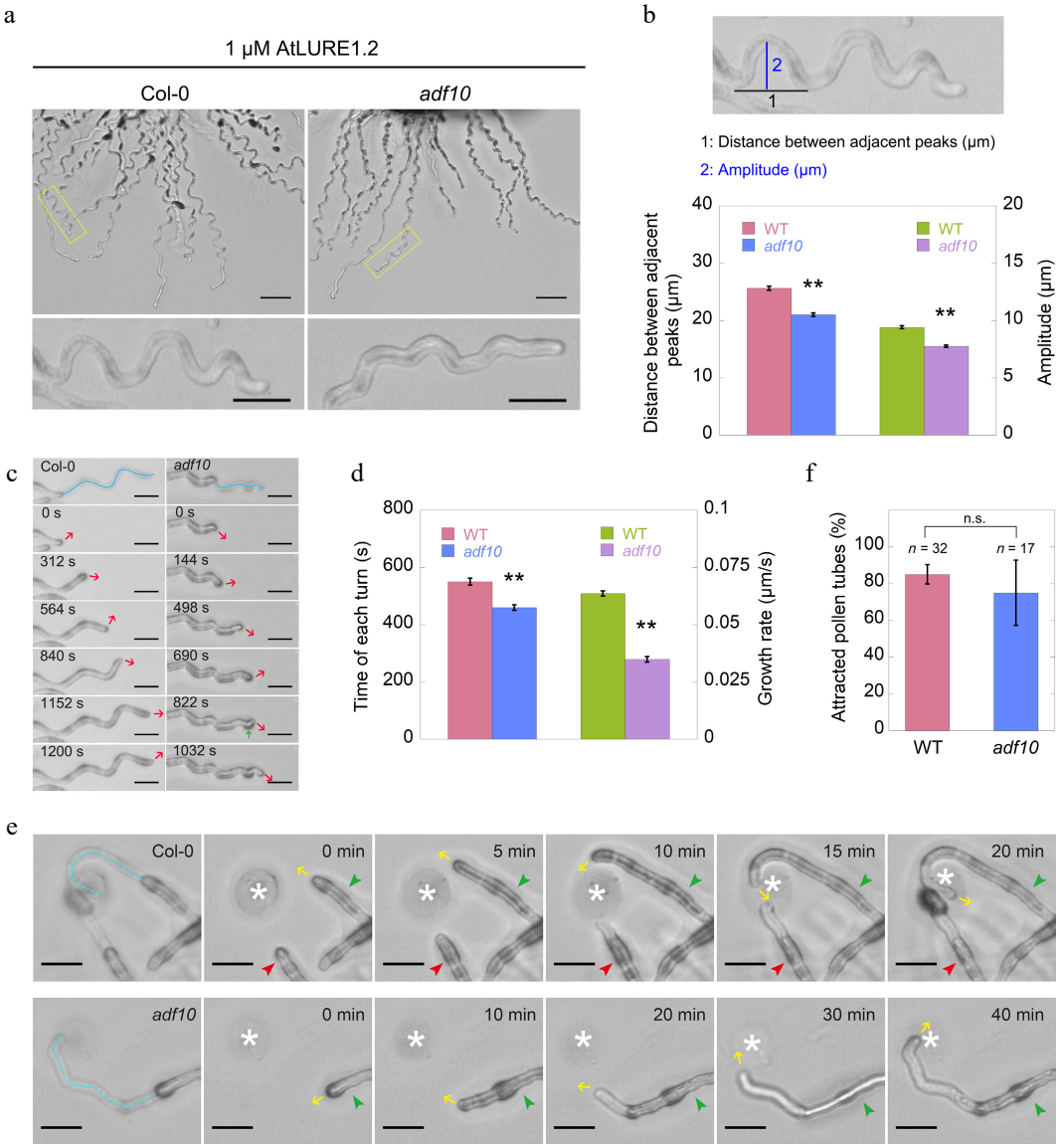

Fig. 2 Loss of function of ADF10 alters AtLURE1.2-induced tube turning behavior. (a) A semi-*in vitro* AtLURE1.2-responsive wavy assay was performed on wild-type (Col-0) and *adf10* mutant pollen tubes. Compared to the wild-type, the pollen tubes of the *adf10* mutant exhibited irregular wavy tip growth on solid GM containing 1 μM AtLURE1.2 peptides. Scale bars, 50 μm (top) and 20 μm (bottom). The micrographs presented are representative of three samples. (b) Quantification of the morphological characteristics of wild-type and *adf10* pollen tubes was conducted. The upper panel depicts a schematic representation of how pollen tube morphology is quantified. The black line represents the distance between adjacent turns, while the blue line indicates the height of one turn. The lower panel displays the quantification results of tube morphology. Data are presented as mean ± SE. ** $p < 0.01$ (Student's *t*-test). (c) and (d) Visualization and quantification of AtLURE1.2-induced tube turning in wild-type and *adf10* mutant pollen tubes were performed. Blue lines in the upper panel of (c) depict the growth track of pollen tubes, red arrows indicate the new growth direction, and the green arrow highlights an abnormal turn in the *adf10* mutant. Data in (d) are presented as mean ± SE. ** $p < 0.01$ (Student's *t*-test). (e) Time-lapse images were captured of WT (upper panel) and *adf10* (lower panel) pollen tubes growing towards AtLURE1.2-beads. The green arrowhead indicates a pollen tube initially growing along the side of an AtLURE1.2-bead, subsequently changing direction to grow towards it. The red arrowhead points to a pollen tube growing straightly towards an AtLURE1.2-bead. Yellow arrows indicate the direction of pollen tube growth. White asterisks mark the position of AtLURE1.2-beads. The entire series of images can be found in Supplemental Videos S1 & S2. Scale bar, 5 μm. (f) Quantification of the percentage of pollen tubes attracted by AtLURE1.2-beads was conducted. Data are presented as mean ± SE. n.s., no significant difference (Student's *t*-test).

Depletion of ADF10 prevents rapid depolymerization of apical actin filaments at the leading side of turning pollen tubes

Next, the aim was to visualize the dynamics of actin filaments in pollen tubes during AtLURE1.2-induced turning. However, a challenge was encountered in that *adf10-1* pollen tubes harboring Lifeact-eGFP grows slowly after navigating through the cut style, thus hindering efforts to visualize actin filament dynamics during their turning. Nevertheless, given that the spatial distribution of actin filaments in pollen tubes during AtLURE1.2-induced turning (see Fig. 1b, c) appeared comparable to that observed in randomly turning pollen tubes growing *in vitro*[39], the focus was shifted to visualize actin dynamics in the turning of pollen tubes growing *in vitro*. In contrast to WT pollen tubes

(Fig. 3, c), it was observed that the apical actin filaments at the leading side of *adf10-1* pollen tubes failed to depolymerize rapidly before the onset of turning (Fig. 3c–e). Furthermore, notably, there was an accumulation of disorganized actin filaments at the leading side of *adf10-1* pollen tubes throughout the entire turning process (Fig. 3c). These findings suggest that the rapid depolymerization of actin filaments, which typically precedes the turning of pollen tubes, is compromised in *adf10-1* pollen tubes. Consequently, this delays the reorganization of the apical actin structure towards the new growth direction.

ADF10 undergoes asymmetric localization during tube turning

To understand how ADF10 regulates actin dynamics during pollen tube turning, we first sought to determine the intracellular localization of ADF10 during this process. Although previous studies have demonstrated that ADF10pro:ADF10-EGFP can complement the growth defects of *in vitro* growing pollen tubes[40], it was unexpectedly found that it cannot fully rescue the pollen tube turning behavior of *adf10-1* in the semi-*in vitro*

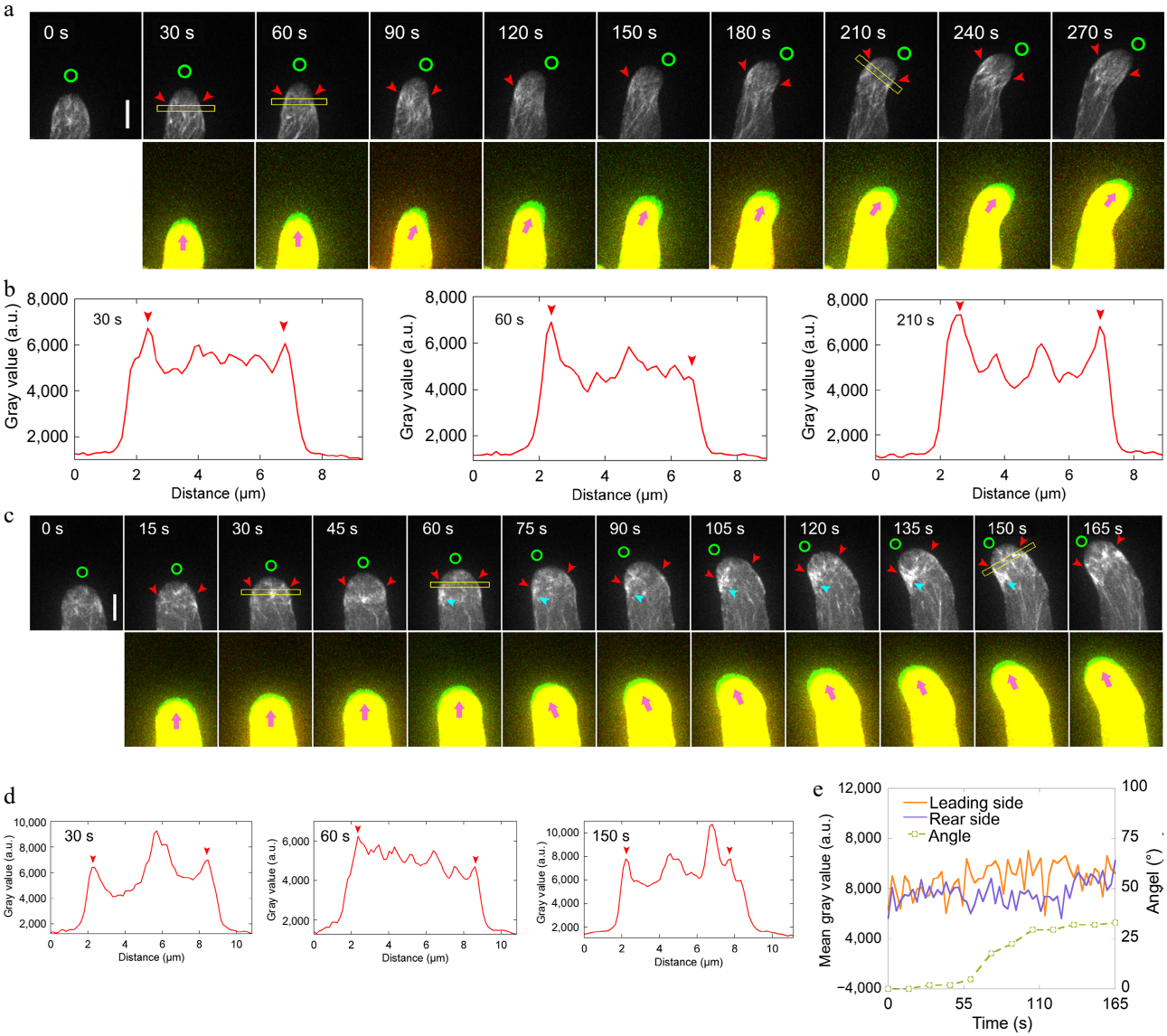

Fig. 3 Loss of function of ADF10 induces accumulation of actin filaments at the leading side in turning pollen tubes growing *in vitro*. (a) Time-lapse images of actin filaments during the turning of *in vitro* growing wild-type pollen tube. The lower panel shows the merged images from two time points, in which the newly grown portion of pollen tubes between two time points was green colored. Green circles in the upper panel and pink arrowheads in the lower panel indicate the new tube growth direction, while red arrowheads in the upper panel highlight the cortical apical actin filaments. Scale bar, 5 μm. (b) Quantification of the fluorescence intensity of apical actin filaments, as indicated by the yellow square in (a). Red arrowheads mark the peaks of fluorescence. (c) Time-lapse images of actin filaments during random turning of an *in vitro* growing *adf10* pollen tube. The lower panel shows the merged images from two time points, in which the newly grown portion of pollen tubes between two time points was green colored. Green circles in the upper panel and pink arrowheads in the lower panel indicate the new tube growth direction, and red arrowheads in the upper panel highlight the cortical apical actin filaments. Scale bar, 5 μm. (d) Quantification of the fluorescence intensity of apical actin filaments, as indicated by the yellow square in (c). Red arrowheads mark the peaks of fluorescence. (e) Analysis of the fluorescence intensity of the pollen tube in (c) on both sides at the region 2.5 to 3.5 μm away from the tip, along with the tube turning angles over time.

AtLURE1.2-responsive assay (Fig. 4a & b). Given that apical actin filaments exhibit a similar organization during both random and AtLURE1.2-guided turning, and considering that ADF10-EGFP is fully functional in rescuing growth defects *in vitro*, the focus was shifted to visualizing the localization of ADF10-EGFP during random turning of pollen tubes growing *in vitro*. The observations revealed that ADF10 is comparatively concentrated in the leading subapex region, precisely where actin filaments undergo rapid depolymerization (Fig. 4c). Specifically, kymograph analysis demonstrated that ADF10 accumulates at the leading side before the turning of the pollen tube and subsequently distributes uniformly at both the leading and rear sides once a new growth direction is established (Fig. 4d, e). These findings strongly suggest that ADF10 undergoes asymmetric localization at the subapex before the turning of the pollen tube.

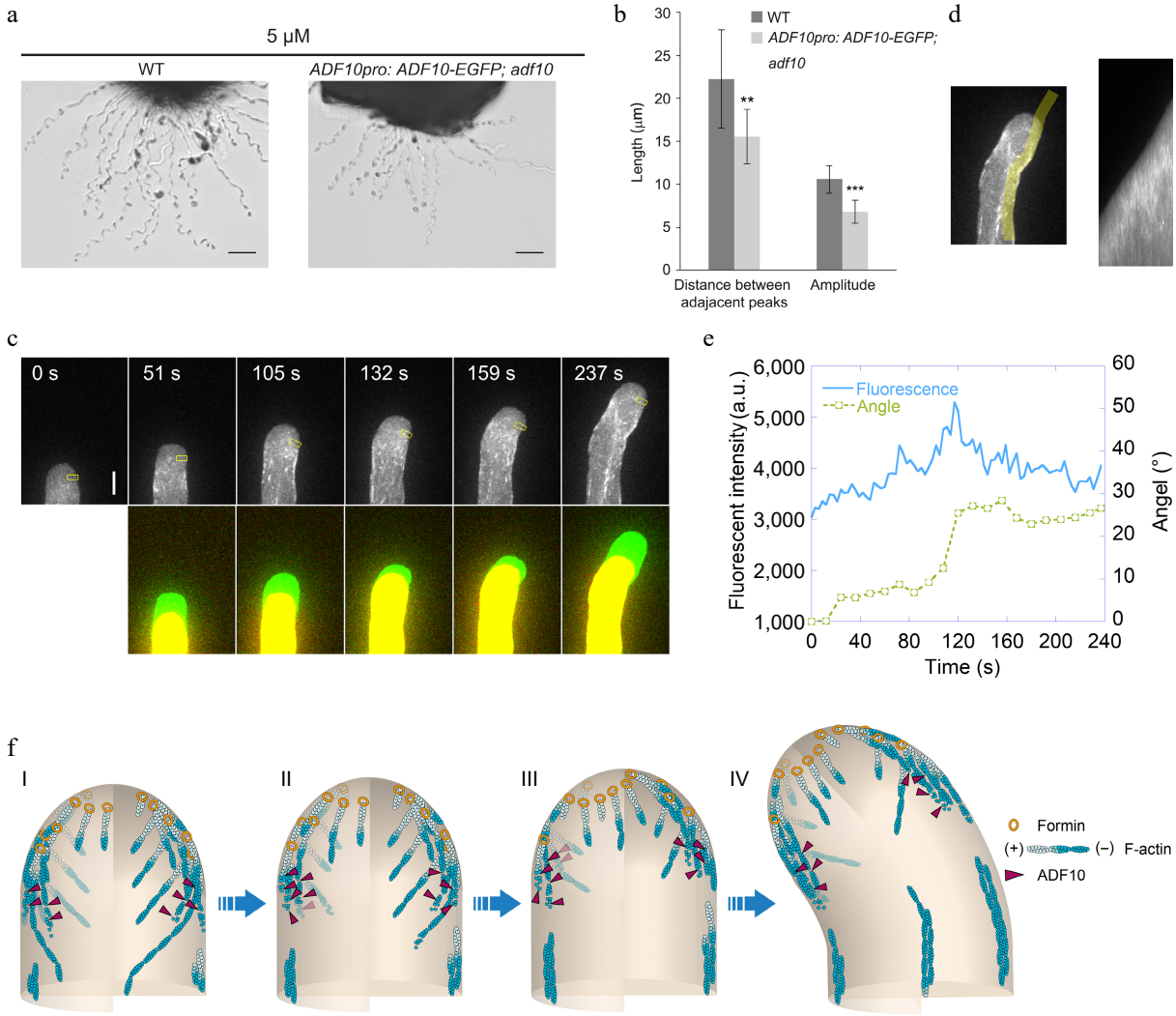

Fig. 4 ADF10 undergoes asymmetric localization during random tube turning. (a) Images of WT and *ADF10pro: ADF10-EGFP* pollen tubes growing out from the cut style. Scale bars, 50 μm. The micrographs are representative of three samples. (b) Quantification of the morphological characteristics of wild-type and *ADF10pro: ADF10-EGFP; adf10* pollen tubes in (a) was conducted. Data are presented as mean ± SE. ** $p < 0.01$ (Student's *t*-test). (c) Time-lapse images of *ADF10pro: ADF10-EGFP* pollen tubes growing *in vitro*. The upper panel shows the time-lapse images. The lower panel shows the merged images from two time points, in which the newly grown portion of pollen tubes between two time points was green colored. Scale bars, 5 μm. (d) The kymograph analysis of ADF10-EGFP in the pollen tube shown in (c). The region of interest used for the kymograph measurement is outlined in the left panel. (e) Analysis of the average fluorescence pixel intensity of apical ADF10-EGFP at the leading side and tube turning angle over time. The fluorescence intensity within the yellow square on the leading side shown in the upper panel of (c), which is 2.5 to 3.5 μm away from the tip, was measured and plotted over time. Meanwhile, the turning angle of the pollen tube was measured and plotted overtime. (f) Schematic depiction of the relationship between apical actin filaments and ADF10 during AtLURE1.2-induced pollen tube turning. At the initial stage, apical actin filaments appear similar on both sides, and ADF10 exhibits a uniform distribution (I). Prior to the onset of pollen tube turning (II and III), ADF10 begins to accumulate at the leading side (IV), resulting in the depolymerization of actin filaments there. Subsequently, repolymerization of apical actin filaments mediated by formins from plasma membrane occurs at the leading side and a new apical actin structure forms, determining the new growth direction of the pollen tube (III). Once the turn is completed, ADF10 returns to a uniform distribution on both sides of the pollen tube tip. Subsequently, the pollen tube grows straight towards the new direction. "+" and "-" refer to the barbed end and pointed end of actin filament, respectively.

Discussion

For the first time, the dynamics of actin filaments in pollen tubes responding to AtLURE1s signaling during their guided growth were directly visualized using a semi-*in vitro* system. The observations revealed that actin filaments undergo initial rapid depolymerization at the leading side, followed by the repolymerization from the plasma membrane to form a new apical actin structure aligned with the growth direction. This process facilitates the turning of the pollen tube. This requirement for rapid depolymerization of actin filaments at the leading side for smooth turning is supported by data showing that depleting ADF10 hinders this depolymerization, delaying the reformation of the apical actin structure in the new direction and impeding the turning of pollen tubes. These findings suggest that the early rapid depolymerization of actin filaments at the leading side is crucial for the reconstruction of the apical actin structure in the new growth direction, a key cellular event in the guided growth of pollen tubes.

During the reorientation of pollen tubes, an asymmetric distribution of ADF10 was noticed, with a slight concentration at the apical leading side before the tube turns (Fig. 4c–e). This distribution pattern likely contributes to ADF10's role in rapidly depolymerizing actin filaments at the leading side of the pollen tube. Future characterization of the localization and function of several ADF cofactors such as CAP1[25] and AIP1[36,48,49], within this context, will further enhance our understanding of how ADF-mediated actin depolymerization contributes to pollen tube turning. Additionally, ADF10 at the leading side might be locally activated by various factors to enhance its depolymerizing activity during turning. For instance, AtLURE1s signaling could activate the membrane-anchored H^+-ATPase[50,51], allowing H^+ to be pumped outside, locally elevating the pH at the subapex. This, in turn, might activate ADF10 to induce actin depolymerization, given that ADF10 prefers a high pH for depolymerizing actin filaments[52]. Furthermore, AtLURE1s signaling might also stimulate Ca^{2+} channels, increasing cytosolic Ca^{2+} concentration, which could directly or indirectly affect the actin-depolymerizing activity of ADF10. Previous studies have shown that Ca^{2+} concentration increases at the leading side during pollen tube turning[53], and active calcium-dependent protein kinase and Ca^{2+} channel CNGC18 relocalizes to this region during reorientation[54,55]. Recent research also indicates that the actin-depolymerizing activity of ADF7 is enhanced by CDPK16-mediated phosphorylation[56]. Whether ADF10 can be similarly activated by Ca^{2+}/CDPK to promote actin depolymerization during pollen tube reorientation remains to be investigated.

The accumulation of actin filaments at the leading side of the subapex might be partly due to increased actin polymerization originating from the apical plasma membrane during the turning of *adf10* pollen tubes. As membrane-derived actin polymerization is controlled by membrane-localized formins[29,57], this suggests that the activity of these formins might be asymmetrically activated in response to upstream AtLURE1s signaling. Formins might redistribute asymmetrically, concentrating at the leading side before pollen tube reorientation. This speculation is inspired by observations showing asymmetric distribution of PRK6 during AtLURE1s signaling perception[4]. In support of this hypothesis, it was found that AtFH5 exhibits slight redistribution on the plasma membrane toward the future growth direction (Supplemental Fig. S5). Additionally, the actin nucleation activity of membrane-localized formins at the leading side might be enhanced after perceiving AtLURE1s signaling for unknown reasons. Moreover, an increase in cytosolic Ca^{2+} concentration likely enhances the actin sequestering activity of profilin as demonstrated previously[58], which promotes the formation of profilin/actin complexes at the leading side of the pollen tube tip. This, in turn, should favor the activity of membrane-localized formins in nucleating actin assembly, as proposed previously[14]. The combination of these factors likely enforces actin polymerization from the membrane at the leading side of the pollen tube, facilitating the formation of a new apical actin structure.

Based on the present findings, it is proposed that the depolymerization and subsequent gradual reassembly of actin filaments at the leading side enable the reconstruction of the apical actin structure, facilitating the turning of pollen tubes (Fig. 4f). Successful turning of pollen tubes relies on the delivery of materials necessary for cell wall synthesis and membrane expansion to the future expanding point. The formation of a new apical actin structure guides the vesicle traffic system to deliver these materials to the expanding point of the pollen tube, facilitating its turning. In support of this hypothesis, previous studies have demonstrated that PRK6, active ROP1, and exocytic vesicles relocate to the intended expansion point of the pollen tube before it turns[4,59–61]. Consistently, exocytosis was shown to play an essential role in the guided growth of pollen tubes in response to external cues[13]. Hence, from the point of this perspective, the guidance of pollen tube is a result of the reorientation of intracellular deliver system that controls pollen tube tip growth. Within this framework, the reconstruction of apical actin structure is an early event to guarantee the redistribution of intracellular trafficking system and successful turning of pollen tubes.

Author contributions

The authors confirm contribution to the paper as follows: study conception and design: Xu Y, Huang S; experiments conduction: Xu Y; data analysis: Xu Y, Jiang J, Huang S; draft manuscript preparation: Xu Y, Huang S; manuscript revision: Huang S. All authors contributed to the discussion of results, manuscript preparation, and approved the final version.

Data availability

All data generated or analyzed during this study are included in this published article and its supplementary information files.

Acknowledgments

We thank the members of the Huang Lab for their insightful discussions. This study was supported by a grant from the National Natural Science Foundation of China (32270338).

Conflict of interest

The authors declare that they have no conflict of interest.

Supplementary Information accompanies this paper at (https://www.maxapress.com/article/doi/10.48130/seedbio-0024-0014)

Dates

Received 16 April 2024; Revised 9 August 2024; Accepted 16 August 2024; Published online 12 September 2024

References

1. Chapman LA, Goring DR. 2010. Pollen-pistil interactions regulating successful fertilization in the Brassicaceae. *Journal of Experimental Botany* 61:1987–99
2. Higashiyama T, Takeuchi H. 2015. The mechanism and key molecules involved in pollen tube guidance. *Annual Review of Plant Biology* 66:393–413
3. Higashiyama T, Yang WC. 2017. Gametophytic Pollen Tube Guidance: Attractant Peptides, Gametic Controls, and Receptors. *Plant Physiology* 173:112–21
4. Takeuchi H, Higashiyama T. 2016. Tip-localized receptors control pollen tube growth and LURE sensing in *Arabidopsis*. *Nature* 531:245–48
5. Wang T, Liang L, Xue Y, Jia PF, Chen W, et al. 2016. A receptor heteromer mediates the male perception of female attractants in plants. *Nature* 531:241–44
6. Okuda S, Tsutsui H, Shiina K, Sprunck S, Takeuchi H, et al. 2009. Defensin-like polypeptide LUREs are pollen tube attractants secreted from synergid cells. *Nature* 458:357–61
7. Takeuchi H, Higashiyama T. 2012. A species-specific cluster of defensin-like genes encodes diffusible pollen tube attractants in *Arabidopsis*. *PLoS Biology* 10:e1001449
8. Zhong S, Liu M, Wang Z, Huang Q, Hou S, et al. 2019. Cysteine-rich peptides promote interspecific genetic isolation in *Arabidopsis*. *Science* 364:eaau9564
9. Meng JG, Zhang MX, Yang WC, Li HJ. 2019. TICKET attracts pollen tubes and mediates reproductive isolation between relative species in Brassicaceae. *Science China Life Sciences* 62:1413–19
10. Guo J, Yang Z. 2020. Exocytosis and endocytosis: coordinating and fine-tuning the polar tip growth domain in pollen tubes. *Journal of Experimental Botany* 71:2428–38
11. Hepler PK, Vidali L, Cheung AY. 2001. Polarized cell growth in higher plants. *Annual Review of Cell and Developmental Biology* 17:159–87
12. Ruan H, Li J, Wang T, Ren H. 2020. Secretory Vesicles Targeted to Plasma Membrane During Pollen Germination and Tube Growth. *Frontiers in Cell and Developmental Biolog* 8:615447
13. Luo N, Yan A, Liu G, Guo J, Rong D, et al. 2017. Exocytosis-coordinated mechanisms for tip growth underlie pollen tube growth guidance. *Nature Communications* 8:1687
14. Zhang R, Xu Y, Yi R, Shen J, Huang S. 2023. Actin cytoskeleton in the control of vesicle transport, cytoplasmic organization, and pollen tube tip growth. *Plant Physiology* 193:9–25
15. Xu Y, Huang S. 2020. Control of the actin cytoskeleton within apical and subapical regions of pollen tubes. *Frontiers in Cell and Developmental Biology* 8:614821
16. Staiger CJ, Poulter NS, Henty JL, Franklin-Tong VE, Blanchoin L. 2010. Regulation of actin dynamics by actin-binding proteins in pollen. *Journal of Experimental Botany* 61:1969–86
17. Chen N, Qu X, Wu Y, Huang S. 2009. Regulation of actin dynamics in pollen tubes: control of actin polymer level. *Journal of Integrative Plant Biology* 51:740–50
18. Cheung AY, Duan QH, Costa SS, de Graaf BHJ, Di Stilio VS, et al. 2008. The dynamic pollen tube cytoskeleton: live cell studies using actin-binding and microtubule-binding reporter proteins. *Molecular Plant* 1:686–702
19. Ren H, Xiang Y. 2007. The function of actin-binding proteins in pollen tube growth. *Protoplasma* 230:171–82
20. Vidali L, Hepler PK. 2001. Actin and pollen tube growth. *Protoplasma* 215:64–76
21. Fu Y. 2015. The cytoskeleton in the pollen tube. *Current Opinion in Plant Biology* 28:111–19
22. Chang M, Huang S. 2015. *Arabidopsis* ACT11 modifies actin turnover to promote pollen germination and maintain the normal rate of tube growth. *The Plant Journal* 83:515–27
23. Zhu L, Zhang Y, Kang E, Xu Q, Wang M, et al. 2013. MAP18 regulates the direction of pollen tube growth in *Arabidopsis* by modulating F-actin organization. *The Plant Cell* 25:851–67
24. Qin T, Liu X, Li J, Sun J, Song L, et al. 2014. *Arabidopsis* microtubule-destabilizing protein 25 functions in pollen tube growth by severing actin filaments. *The Plant Cell* 26:325–39
25. Jiang Y, Chang M, Lan Y, Huang S. 2019. Mechanism of CAP1-mediated apical actin polymerization in pollen tubes. *Proceedings of the National Academy of Sciences of the United States of America* 116:12084–93
26. Wu Y, Yan J, Zhang R, Qu X, Ren S, et al. 2010. *Arabidopsis* FIMBRIN5, an actin bundling factor, is required for pollen germination and pollen tube growth. *The Plant Cell* 22:3745–63
27. Li S, Dong H, Pei W, Liu C, Zhang S, et al. 2017. LlFH1-mediated interaction between actin fringe and exocytic vesicles is involved in pollen tube tip growth. *New Phytologist* 214:745–61
28. Su H, Zhu J, Cai C, Pei W, Wang J, et al. 2012. FIMBRIN1 is involved in lily pollen tube growth by stabilizing the actin fringe. *The Plant Cell* 24:4539–54
29. Lan Y, Liu X, Fu Y, Huang S. 2018. *Arabidopsis* class I formins control membrane-originated actin polymerization at pollen tube tips. *PLoS Genetics* 14:e1007789
30. Wang HJ, Wan AR, Jauh GY. 2008. An actin-binding protein, LlLIM1, mediates calcium and hydrogen regulation of actin dynamics in pollen tubes. *Plant Physiology* 147:1619–36
31. Xiang Y, Huang X, Wang T, Zhang Y, Liu Q, et al. 2007. ACTIN BINDING PROTEIN29 from *Lilium* pollen plays an important role in dynamic actin remodeling. *The Plant Cell* 19:1930–46
32. Liu X, Qu X, Jiang Y, Chang M, Zhang R, et al. 2015. Profilin regulates apical actin polymerization to control polarized pollen tube growth. *Molecular Plant* 8:1694–709
33. Zhu J, Nan Q, Qin T, Qian D, Mao T, et al. 2017. Higher-ordered actin structures remodeled by *Arabidopsis* ACTIN-DEPOLYMERIZING FACTOR5 are important for pollen germination and pollen tube growth. *Molecular Plant* 10:1065–81
34. Jiang Y, Lu Q, Huang S. 2022. Functional non-equivalence of pollen ADF isovariants in Arabidopsis. *The Plant Journal* 110:1068–81
35. Chen CY, Wong EI, Vidali L, Estavillo A, Hepler PK, et al. 2002. The regulation of actin organization by actin-depolymerizing factor in elongating pollen tubes. *The Plant Cell* 14:2175–90
36. Diao M, Li X, Huang SJ. 2020. *Arabidopsis* AIP1-1 regulates the organization of apical actin filaments by promoting their turnover in pollen tubes. *Science China-Life Sciences* 63:239–50
37. Zhang R, Qu X, Zhang M, Jiang Y, Dai A, et al. 2019. The Balance between Actin-Bundling Factors Controls Actin Architecture in Pollen Tubes. *iScience* 16:162–76
38. Zheng Y, Xie Y, Jiang Y, Qu X, Huang S. 2013. *Arabidopsis* ACTIN-DEPOLYMERIZING FACTOR7 severs actin filaments and regulates actin cable turnover to promote normal pollen tube growth. *The Plant Cell* 25:3405–23
39. Qu X, Zhang R, Zhang M, Diao M, Xue Y, et al. 2017. Organizational innovation of apical actin filaments drives rapid pollen tube growth and turning. *Molecular Plant* 10:930–47
40. Jiang Y, Wang J, Xie Y, Chen N, Huang S. 2017. ADF10 shapes the overall organization of apical actin filaments by promoting their turnover and ordering in pollen tubes. *Journal of Cell Science* 130:3988–4001
41. Wang ZP, Xing HL, Dong L, Zhang HY, Han CY, et al. 2015. Egg cell-specific promoter-controlled CRISPR/Cas9 efficiently generates homozygous mutants for multiple target genes in *Arabidopsis* in a single generation. *Genome Biology* 16:144

42. Clough SJ, Bent AF. 1998. Floral dip: a simplified method for *Agrobacterium*-mediated transformation of *Arabidopsis thaliana*. *The Plant Journal* 16:735–43
43. Hamamura Y, Nishimaki M, Takeuchi H, Geitmann A, Kurihara D, et al. 2014. Live imaging of calcium spikes during double fertilization in *Arabidopsis*. *Nature Communications* 5:4722
44. Boavida LC, McCormick S. 2007. Temperature as a determinant factor for increased and reproducible *in vitro* pollen germination in *Arabidopsis thaliana*. *The Plant Journal* 52:570–82
45. Qu X, Zhang H, Xie Y, Wang J, Chen N, Huang S. 2013. *Arabidopsis* villins promote actin turnover at pollen tube tips and facilitate the construction of actin collars. *The Plant Cell* 25:1803–17
46. Vidali L, Rounds CM, Hepler PK, Bezanilla M. 2009. Lifeact-mEGFP reveals a dynamic apical F-actin network in tip growing plant cells. *PLoS One* 4:e5744
47. Zhang M, Zhang R, Qu X, Huang S. 2016. Arabidopsis FIM5 decorates apical actin filaments and regulates their organization in the pollen tube. *Journal of Experimental Botany* 67:3407–17
48. Shi M, Xie Y, Zheng Y, Wang J, Su Y, et al. 2013. *Oryza sativa* actin-interacting protein 1 is required for rice growth by promoting actin turnover. *The Plant Journal* 73:747–60
49. Ketelaar T, Allwood EG, Anthony R, Voigt B, Menzel D, et al. 2004. The actin-interacting protein AIP1 is essential for actin organization and plant development. *Current Biology* 14:145–49
50. Chen W, Jia PF, Yang WC, Li HJ. 2020. Plasma membrane H^+-ATPases-mediated cytosolic proton gradient regulates pollen tube growth. *Journal of Integrative Plant Biology* 62:1817–22
51. Hoffmann RD, Portes MT, Olsen LI, Damineli DSC, Hayashi M, et al. 2020. Plasma membrane H(+)-ATPases sustain pollen tube growth and fertilization. *Nature Communications* 11:2395
52. Wang J, Shen J, Xu Y, Jiang Y, Qu X, et al. 2023. Differential sensitivity of ADF isovariants to a pH gradient promotes pollen tube growth. *The Journal of Cell Biology* 222:e202206074
53. Malhó R, Trewavas AJ. 1996. Localized apical increases of cytosolic free calcium control pollen tube orientation. *The Plant Cell* 8:1935–49
54. Moutinho A, Trewavas AJ, Malho R. 1998. Relocation of a Ca^{2+}-dependent protein kinase activity during pollen tube reorientation. *The Plant Cell* 10:1499–509
55. Meng JG, Liang L, Jia PF, Wang YC, Li HJ, et al. 2020. Integration of ovular signals and exocytosis of a Ca^{2+} channel by MLOs in pollen tube guidance. *Nature Plants* 6:143–53
56. Wang Q, Xu Y, Zhao S, Jiang Y, Yi R, et al. 2023. Activation of actin-depolymerizing factor by CDPK16-mediated phosphorylation promotes actin turnover in *Arabidopsis* pollen tubes. *PLoS Biology* 21:e3002073
57. Cheung AY, Niroomand S, Zou Y, Wu HM. 2010. A transmembrane formin nucleates subapical actin assembly and controls tip-focused growth in pollen tubes. *Proceedings of the National Academy of Sciences of the United States of America* 107:16390–95
58. Kovar DR, Drøbak BK, Staiger CJ. 2000. Maize profilin isoforms are functionally distinct. *The Plant Cell* 12:583–98
59. Hwang JU, Gu Y, Lee YJ, Yang Z. 2005. Oscillatory ROP GTPase activation leads the oscillatory polarized growth of pollen tubes. *Molecular Biology of the Cell* 16:5385–99
60. Bove J, Vaillancourt B, Kroeger J, Hepler PK, Wiseman PW, et al. 2008. Magnitude and direction of vesicle dynamics in growing pollen tubes using spatiotemporal image correlation spectroscopy and fluorescence recovery after photobleaching. *Plant Physiology* 147:1646–58
61. Bou Daher F, Geitmann A. 2011. Actin is Involved in Pollen Tube Tropism Through Redefining the Spatial Targeting of Secretory Vesicles. *Traffic* 12:1537–51